

# HIGH POWER TARGET INSTRUMENTATION AT J-PARC FOR NEUTRON AND MUON SOURCES

Shin-ichiro Meigo\*, Motoki Ooi, Kiyomi Ikezaki, Tomoyuki Kawasaki, Hidetaka Kinoshita, Atsushi Akutsu, Masaaki Nisikawa and Shinpei Fukuta, J-PARC center, JAEA, 319-1195, Japan  
Hiroshi Fujimori, J-PARC center, KEK, 305-0801, Japan

## Abstract

Since 2008, the Japanese Spallation Neutron Source (JSNS) of J-PARC has produced a high-power proton beam of 300 kW. In order to operate with high intensity beam such as 1 MW, a reliable beam instruments are crucial. We developed profile monitor system by using SiC as sensor wires. Since pitting erosion was found at the vessel of the spallation neutron target at other facility of SNS, the beam current density at the target should be kept as low as possible. To decrease the beam current density at the target, a beam flatterer system based on a non-linear optics with octupole magnets was developed. Beam profile at the target obtained with the Multi Wire Profile Monitor (MWPM) showed flat distribution and showed good agreement with the design calculation. Furthermore, the present status of the development of the beam instruments are also described.

## INTRODUCTION

In the Japan Proton Accelerator Research Complex (J-PARC) [1], a MW-class pulsed neutron source, the Japan Spallation Neutron Source (JSNS) [2], and the Muon Science facility (MUSE) [3] will be installed in the Materials and Life Science Experimental Facility (MLF) shown in Fig. 1. In 2015, we successfully ramped up beam power to 500 kW continuously<sup>1</sup> and delivered several shots of the 1-MW beam to the targets. To produce a neutron source, a 3 GeV proton beam collides with a mercury target, and to produce a muon source, the 3 GeV proton beam collides with a 2-cm-thick carbon graphite target. To efficiently use the proton beam for particle production, both targets are aligned in a cascade scheme, with the graphite target placed 33 m upstream of the neutron target. For both sources, the 3 GeV proton beam is delivered from a rapid cycling synchrotron (RCS) to the targets by the 3NBT (3 GeV RCS to Neutron facility Beam Transport) [4–6]. Before injection into the RCS, the proton beam is accelerated up to 0.4 GeV by a LINAC. The beam is accumulated in two short bunches and accelerated up to 3 GeV in the RCS. The extracted 3 GeV proton beam, with a 150 ns bunch width and a spacing of 600 ns, is transferred to the muon production target and the spallation neutron source.

Recently, pitting damage became evident in the mercury target container [7], and the extent of the damage is proportional to the fourth power of the peak current density of the proton beam. After operating the beam at high power, sig-

nificant pitting damage was observed at the spent mercury target vessel at JSNS and at the Spallation Neutron Source (SNS) in Oak Ridge National Laboratory [8, 9]. Using linear optics (i.e., quadrupole magnets) for beam transport, the peak current density can be reduced by expanding the beam at the target. However, beam expansion increases heat in the vicinity of the target, where shielding and the neutron reflector are located. Therefore, the peak current density is limited by the heat induced in the vicinity of the target. At the JSNS, the minimum peak current density is expected to be  $9 \mu\text{A}/\text{cm}^2$ , which gives a thermal energy density at the target of  $14 \text{ J}/\text{cm}^3/\text{pulse}$  [10]. Because the pitting damage goes as the fourth power of the peak density, scanning the beam with a deflecting magnetic field will not mitigate the pitting damage.

Beam profile monitoring plays an important role in comprehending the damage to the target. Therefore it is very important to watch continuously the status of the beam at the target at the JSNS especially for the peak current density. We have developed a reliable beam profile monitor for the target by using Multi Wire Profile Monitor (MWPM). In order to watch the two dimensional profile on the target, we have also developed the profile monitor based on the imaging of radiation of the target vessel after beam irradiation. In this paper, the present status of the beam monitor at the spallation neutron source is described.

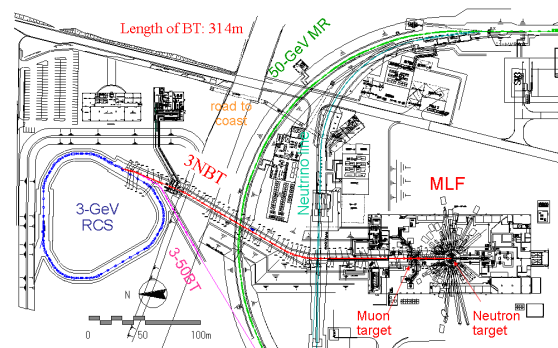


Figure 1: Plan of rapid cycling synchrotron (RCS) at the Materials and Life Science Experimental Facility (MLF) at J-PARC.

## BEAM MONITOR SYSTEM AT THE BEAM TRANSPORT TO THE TARGET

### Silicon Carbide Sensor Wire

In order to obtain the characteristics of the proton beam, diagnostic system based on a Multi Wire Profile Monitor

\* meigo.shinichiro@jaea.go.jp

<sup>1</sup> Recently the power is restricted to 200 kW due to no spare mercury target remaining since February 2016.

(MWPM) was developed. Principle of the MWPM is simple to observe the amount of the electron emission by the interaction of the beam at the wire. As a material of sensitive wire, usually tungsten wire is selected due to large emission amount of the electron and having high temperature melting point. In the present system, silicon carbide (SiC) was chosen due to the high resistance of the radiation [11], which can survive for 80 DPA. Due to the interaction, the beam loss is caused, which is one of issues of the high intensity proton accelerator and the optimization of the beam loss is important. The angular differential cross section of Rutherford scattering is proportional to square of atomic number of wire material. Therefore wire material with low atomic number has advantage for beam loss. Since the average atomic number of SiC is 10, the differential cross section of SiC becomes 1/55 times of the cross section of tungsten. In order to obtain the angular distribution after scattered by the wire is calculated with revised DECAY-TURTLE [12] by Paul Scherrer Institute (PSI) [13]. It was recognized that SiC wire than tungsten gives less influence on the beam. In order to estimate of the lifetime of monitor wire, the displacement cross section of DPA is calculated with NMTC/JAM [14]. By the calculation, it is found that the DPA cross section of SiC and tungsten for 3-GeV proton is 278 and 7997 b respectively, which shows that DPA of the tungsten is about 29 times larger than SiC. SiC was chosen as wire of as a standard model of the profile monitor at the 3NBT.

### Multi Wire Profile Monitor

The view of MWPM is shown in Fig. 2. Along the beam transport line, 15 sets of movable MWPMs are placed to measure the beam profile. The MWPM frame has 31 wires of SiC with the spacing pitch of 6 mm for each horizontal and vertical direction. We employed the SiC wire having diameter of 0.1 mm, which has a tungsten core of 0.01 mm and is coated with  $1\ \mu\text{m}$  of pyrolytic carbon. The wire frame made of aluminum oxide with purity more than 95 % is selected due to the high radiation resistance. In order to sustain with the fixed tension, wires are kept by the holder with spring, which gives the unique tension of 0.6 N to the wire. The frame of wires is placed in the vacuum chamber made of titanium, which is selected by the following reason, good vacuum characteristics and low activation. In order to avoid unnecessary irradiation of the wires, the frame can retract and moves like the pendulum motion.

For the actual high intensity beam tuning, it is important to know the beam parameter. The intrinsic parameters of the beam transport was confirmed by observing response of beam position for the kick angle of the steering magnet. By the observation of the beam width with the MWPMs, the Twiss parameter and the beam emittance can be acquired with help of the SAD [15] code.

### Monitors Placed at Proton Beam Window

It is very important that continuously observation of the characteristics of the proton beam introduced to the target. Due to the high activations caused by the neutron produced

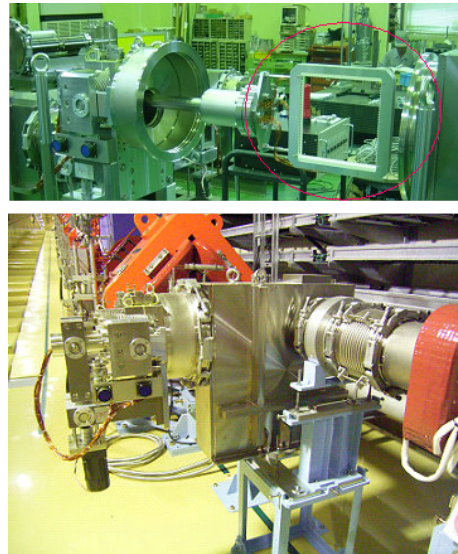


Figure 2: MWPM placed at the beam transport line. (top: MWPM and frame inside the vacuum chamber. Red circle stands for sensor wire head. bottom: MWPM and chamber placed in the beam transport line.)

at the target, remote handling technique is necessary to exchange the beam monitor for the target. In order to decrease the radiation produced at the spallation neutron target, shielding above the monitor was required. To decrease the difficulties of the exchange work and decrease of the shielding, we combined the beam monitors with a Proton Beam Window (PBW) for separation between the vacuum region of the accelerator and the helium region around the neutron target. The PBW is better to be placed closer to the target where distance between the target and the PBW is 1.8 m, which gives reliable profile at the target. In Fig. 3, the MWPM placed at the center of vacuum chamber of the PBW is shown. In order to avoid exceed heat at target vicinities, beam halo monitors are placed as well. The chamber of the PBW has inflatable vacuum seal called pillow seal. Due to the pillow seal, the monitors can be changed by the remote handling. To calibrate sensitivity of each wire, the signal was observed by the scanning the position with narrow width beam. It was found that the difference of individual sensitivity was 6 % at most.

In an actual beam operation, the heat at the target vicinities such as shielding, which mainly does not have water cooling channel, is important for reduction the peak density. Beam halo monitors attached at the PBW to observe the heat deposition at the target vicinities such as reflector and shielding, which is not allowed to exceed  $1\ \text{W}/\text{cm}^3$ . We placed two types of beam halo monitors to obtain the thermal information by thermocouple and the emission of electron by electrode. Since the emission of electron indicates relative intensity of the beam halo, the beam halo relative intensity, which can be normalized by the following thermal observation, can be obtained by several shots of the beam. To observe the absolute intensity of the halo, the thermocou-

ple type was implemented, which consists of copper strips coupled with the thermocouple. With 5 minutes of 25 Hz beam operation, the absolute intensity of the beam halo can be determined by the differential of temperature by time. These procedure was normally performed in actual beam operation.

Since wires at the MWPM placed at the PBW are fixed type and continuously irradiated to the beam, long lifetime wire is required. The profile monitor at the PBW is important so that a redundant system using SiC and tungsten wires was applied. In summer of 2013, some spots were observed at the surface of helium side of the PBW, which were thought to be produced by the erosion of nitric acid produced by the radiolysis around the target. We decided to change the 1st PBW already received the integration beam power of 2000 MWh to the new one. Until 2000 MWh, the wires still gave normal signals and after irradiation they were not found serious damage by inspection.

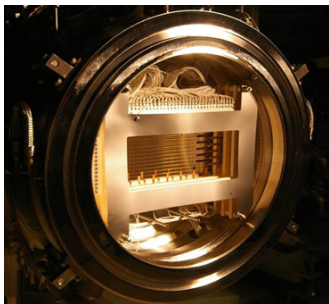


Figure 3: MWPM and beam halo monitors placed at the Proton Beam Window (PBW).

All signals of MWPM is transfer to the local control room by twisted pare cables with high radiation harding. As for the MWPM of the PBW, Mineral Insulator Cables (MICs) are applied because the cables receives quite high radiation does more than 1 MGy. The signal is fed to the inverter amp (Technoland N-GK 160 32ch Inverter AMP) and fed to the charge collective ADC (Technoland C-TS 301B) with the integration time range of 3  $\mu$ s, which has integration charge range of -3 nC in total and is driven by the CAMAC bus. The signals on the CAMAC bus are read out via crate controller of Toyo CC/NET. All signals is controlled by the EPICS [16] and is data base server based on PSQL server. Each result of the beam profile is fitted by the Gaussian and base distribution for every second. Result of the center position and the width is utilized to watch the status of beam injected to the target.

For the safety, if any anomaly of the beam was found such as offset of the beam position, the beam should be immediately. The machine protect system (MPS) was developed, which cut out the beam immediately if either the beam position exceeded 5 mm offset or the beam peak density exceeded the threshold giving the peak heat density of 14 J/cm<sup>3</sup>/pulse at the mercury target. Due to the MPS, high power beam operation such as 1 MW can be performed with high confident. Data of the beam profile for every shots are

watched by the control system driven by the EPICS and are stored in data base.

## DEVELOPMENT OF BEAM FLATTERING SYSTEM USING NON-LINEAR BEAM OPTICS

Distribution of the beam extracted from the RCS can be described well by a simple Gaussian [6]. For the beam with Gaussian distribution in the phase space, the beam profile becomes a Gaussian at all place with an ordinary linear beam optics. By using non-linear optics, the beam particles located at the edge is bent to the center so that the distribution can become flat. In order to obtain flat shape for each horizontal and vertical direction, two octupole magnets is required. These octupole magnets can be placed at anywhere upstream of the target except the place where the phase advance between the magnet and the mercury target is an integer multiple of  $\pi$ . Since the targets had been irradiated by the beam for 5 years, the radiation dose around the targets is too high to place magnet. Therefore, two octupole magnets (OCT1, OCT2) are placed at upstream of the muon target as shown in Fig. 4.

In briefly, the fundamental of the beam flatterng is based on the edge folding by the high order magnet of octupole magnet. By choosing appropriate octupole magnetic field, a flat beam distribution can be obtained as shown in Fig. 5.

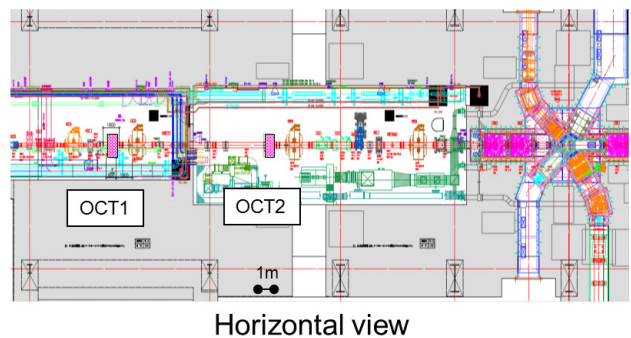


Figure 4: Plan of octupole magnets for beam flattening system, which is to be placed upstream of muon production target shown in right side.

### Beam Optics for Flattering System

In order to achieve flat distribution, the required octupole field is proportional to the inverse square of the beta functions at the octupole magnet. Due to the relative high momentum of the present beam, achievement of a large octupole field of the K is difficult. To obtain the flat shape with the realistic K of the octupole, we expand the beam at the octupole magnet to have large  $\beta$  function. Around the octupole magnet, since physical aperture of quadrupole magnets was fixed to 300 mm, the aperture of the octupole magnet is determined to 300 mm. The admittance of the beam was designed to have 324  $\pi$  mm mrad, which was given by the



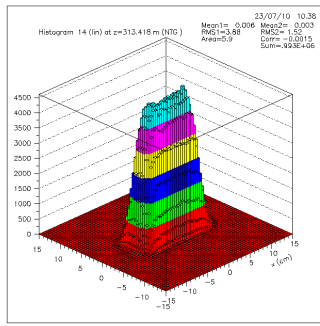


Figure 5: Flat beam distribution at the mercury target by using two set of octupole magnets.

beam collimator placed at the RCS. A study of the RCS [17] showed that the transverse emittance will be as small as  $250 \pi$  mm mrad. The beam admittance at the octupole was determined to  $250 \pi$  mm mrad and the beta function at the octupole magnets was chosen to 200 m.

### Octupole Magnets

Based on the optics design, two pieces of the octupole magnet shown in Fig. 6 were fabricated. The designed field gradient is  $800 \text{ T/m}^3$  with a bore diameter of 0.3 m and 0.6 m in length of pole and the current of 700 A. Using a hall probe, the field gradient was measured. It was confirmed that the magnetic field were in good agreement with the design calculation. In an actual beam operation, the beam centering at the octupole is important to avoid peak at the edge. To perform centering, beam position monitor was installed in each octupole magnet.

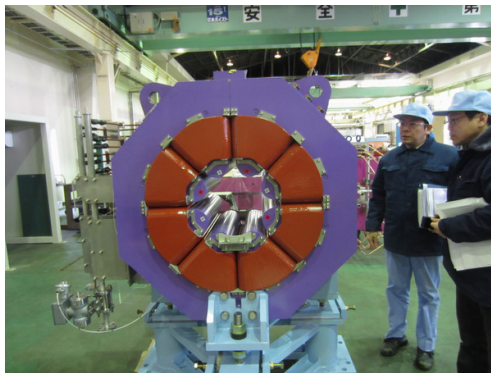


Figure 6: Fabricated octupole magnet with magnetic field gradient of  $800 \text{ T/m}^3$ .

### Beam Profile with Non-linear Optics

In order to obtain the beam profile at the neutron source, SAD code is utilized, which provide beam information by fitting the result given by the MWPM placed at upstream of the octupole magnet. Also revised DECAY-TURTLE [12] by Paul Scherrer Institute (PSI) [13] is utilized to simulate multiple scattering at the muon target. Figure 7 shows results of beam profile for 800 kW beam with and without excitation

of the octupole magnets. The beam profile shown in Fig. 7 was observed by the MWPM placed at the PBW. It can be found that considerable flat distribution can be obtained by the non-linear optics. The calculation results with and without excitation are also shown in Fig 7. The calculation results show good agree with the experiment ones with and without octupole magnetic field. It is also confirmed that the calculated beam profile by using the muon target showed good agreement with the experiment for both cases with and without octupole magnetic field. By the calculation result, the peak density can be thought to be reduced by 30% compared with the linear optics.

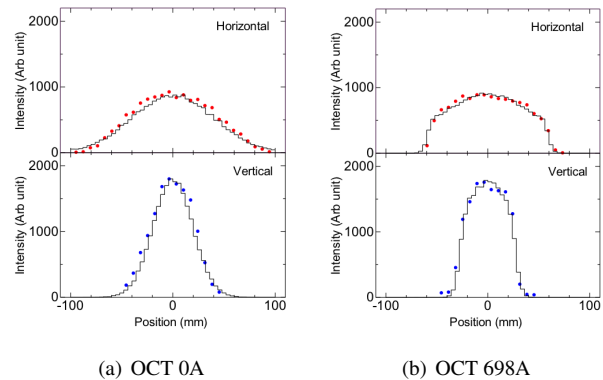


Figure 7: Beam profile obtained with calculations (line) compared with result by the MWPM (dots) supplying current of (a) 0 A and (b) 698 A to octupole magnet. Upper and bottom figure represents for horizontal and vertical directions, respectively.

## DEVELOPMENT NEW BEAM INSTRUMENTS

### Lifetime Estimation of the PBW

The MWPM placed at the PBW so that the lifetime estimation of the PBW is important. When the water was leaked from the PBW, enormous efforts and time will be necessary for restoring. If water leaked from the PBW to the vacuum side, the baking procedure will be necessary to reduce the outgas inside vacuum. We chose aluminum alloy as the material of the PBW, because SINQ at PSI had a good result for lifetime as a safety hull material of the target. Post irradiation examination (PIE) was already performed and material property was studied preciously at the SINQ [18]. The lifetime can be thought to be determined by the embrittlement due to the especially helium caused by the spallation reaction. Therefore, helium production rate is important to estimation of the lifetime. To eliminate difference of the proton energy, calculation should be made for He production rate for the proton energy, whereas the SINQ is utilized 590-MeV protons. In order to obtain validate of nuclide production, cross section for residual nuclide was measured using 3-GeV proton with thin aluminum foil (0.5 mm) placed at front of the beam dump. The gamma

ray caused by the residual nuclide was observed with High Pure Germanium (HP-Ge) detector. Due to high intensity beam, irradiation time was enough to 5 min. Figure 8 shows obtained cross section for  $^{27}\text{Al}(p,x)^7\text{Be}$  reaction compared with other experiment [19–21], calculation code [14] and evaluated nuclear data [22]. It is shown that experimental data with relatively high accuracy can be obtained by well controlled beam and beam monitors with high precision. Using 3-GeV result, calculation code for H and He gas production may be improved. By using developed code, a reliable lifetime of the PBW will be obtained.

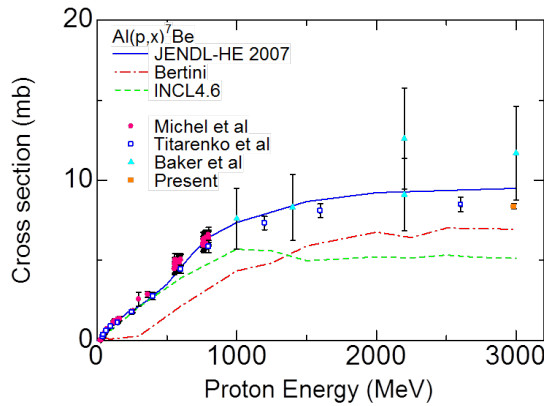


Figure 8: Experimental result of  $^{27}\text{Al}(p,x)^7\text{Be}$  reaction for code validation.

### Development of New Profile Monitor

Until now the monitor wire survived up to 2 GWh, which was at attached the first PBW, however, there is no evidence that the MWPM will survive for long duration of 1 MW beam. The lifetime of the PBW is expected as 2 years for 1 MW beam [23], which has proton fluence  $2 \times 10^{21} \text{ cm}^{-2}$  and the integral beam power of 10 GWh. Furthermore, a target material experimental facility for accelerator driven system (ADS) is planned at J-PARC, where the peak current density will be 5 times higher than the MLF [24]. In order to observe 2D profile, a on-line type profile monitor is desired because the present 2D beam profile by IP can be obtained after the irradiation. Therefore we began to develop a new beam profile monitors.

By observation of the thermal distribution at the target, the beam profile can be obtained. We developed an infrared camera system with bundled hollow-core fibers having length of 1 m. The hollow-core fibers were made of the quartz capillary-tube coated by polyimide. Since beam monitor is placed at the PBW, the radiation hardening of the monitor is required obviously. The capillary tube is made of inorganic material and the camera can be placed far away from the radiation source so that the infrared system can be thought to have enough high radiation hardening.

Also we developed a profile monitor based on the bundled optical fibers with high radiation hardening (Fujikura FISR-

20) having  $2 \times 10^4$  pixels and length of 5 m. By painting fluorescence material such as alumina at the target vessel, the beam profile can be observed with fluorescence, which already utilized at the SNS. In future, we will place the present fiber system at the PBW.

To observe temperature anomaly on the target, the image of fibers was obtained with the near infrared filter to cut the visible light. Figure 9 shows the direct image of the near infrared from the ceramic heater as the system demonstration. The present near infrared system may be utilized for diagnostic system of the muon production target. Since the muon production target was the rotating target cooled by the radiation heat having any cooling channel, if the rotation stopped by certain cause then the temperature will arise rapidly eventually introduce break of the target. Due to the rotation target, observation of the temperature by the thermocouple was difficult. Normally the temperature of the target exceeded  $1000 \text{ }^\circ\text{C}$  so that By the near infrared system, the anomaly of the target can be easily detected.

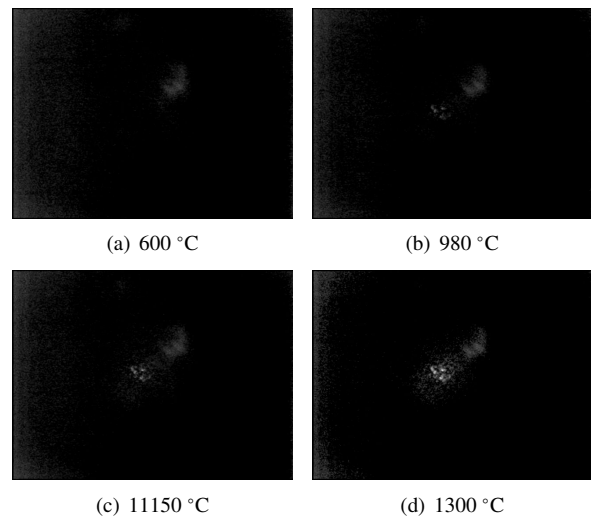


Figure 9: Images obtained by the near infrared beam profile system for various temperature of ceramic heater.

### CONCLUSION

For reliable beam operation at the JSNS in J-PARC, beam instruments have been developed. By using the MWPM, beam parameter such as the emittance and Twiss parameter can be obtained by several shots of the beam. Under the present system, high power beam operation such as 1 MW can be performed with high confident.

In order to reduce peak density of the beam current at the target, a non-linear beam optics with the octupole magnets was developed. By the present system, it was found that the flat shape can be obtained. The calculation simulation shows good agreement with the result obtained with the present profile monitor, which implies that the beam flattening can be achieved by the design of optics having large  $\beta$  function at the octupole magnet and an appropriate phase advance between the octupole and the mercury target. By the cal-

ulation including with the beam scattering on the muon production target, it is shown that the peak current density can be reduced about 30 % of the peak density without the non-linear beam optics.

## ACKNOWLEDGMENT

This work is partly supported by the Ministry of Education, Culture, Sports, Science and Technology (MEXT) KAKENHI Grant-in-Aid for Scientific Research (C) Grant no. 26390114.

## REFERENCES

- [1] The Joint Project Team of JAERI and KEK, JAERI-Tech 99-56, 1999.
- [2] Y. Ikeda, Nucl. Instrum. Meth. **A600**, (2009) 1.
- [3] Y. Miyake, et al., Physica B **404** (2009) 957.
- [4] S. Meigo, et al., Nucl. Instrum. Meth. **A562**, (2006) 569.
- [5] S. Sakamoto, et al., Nucl. Instrum. Meth. **A562**, (2006) 638.
- [6] S. Meigo, et al., Nucl. Instrum. Meth. **A600**, (2009) 41.
- [7] M. Futakawa, et al., J. Nucl. Sci. Technol. **40** (2004) 895.
- [8] T. Naoe, et al., J. Nucl. Mater. **450** (2014) 123.
- [9] D. A. McClintock, et al., J. Nucl. Mater., **431** (2012) 147.
- [10] S. Meigo, et al., MOPEB066, IPAC10 (2010).
- [11] G. E. Youngblood, et al., J. Nucl. Mater. , **258 - 263**, 1551 (1998).
- [12] K.L. Brown, Ch. Iselin and D.C. Carey: Decay Turtle, CERN 74-2 (1974).
- [13] PSI Graphic Turtle Framework by U. Rohrer based on a CERN-SLAC-FERMILAB version.
- [14] K. Niita, et al., JAERI-Data/Code 2001-007 (2001).
- [15] K.Oide, et al, Phys. Rev. E **49** , 4474 (1994).
- [16] M. Ooi, et al., PO1.024-1, ICALEPCS10 (2005).
- [17] H. Hotchi, et al., THPPP080, IPAC12 (2012).
- [18] Y. Dai, et al., J. Nucl. Mater., **343**, 184 (2005).
- [19] Yu.E.Titarenko, et al., Yadernaya Fizika Vol. **74**, 531 (2011).
- [20] R. Michel, et al., Nucl. Instrum. Meth. Phys. Res., Sect. B **129**, 153 (1997).
- [21] E.Baker, et al., Phys. Rev. **112**, 1319 (1958).
- [22] Y. Watanabe, et al., J. Korean Phys. Soc. **59**, 1040 (2011).
- [23] S. Meigo, et al., J. Nucl. Mater. , **450**, 141 (2014).
- [24] S. Meigo, et al., J. Nucl. Mater. , **450**, 8 (2014).